

Visualization in a water channel as a preliminary design tool

BARCALA-MONTEJANO, M.A. *, RODRÍGUEZ-SEVILLANO, A.A. *, DELGADO-OBREGÓN, C. **

* Professors at the UPM (Technical University of Madrid), Madrid, Spain.

** Mrs. Delgado, C. (Bachelor by Technical University of Madrid), Spain.

Abstract

This paper presents the visualization results obtained in a water channel. These results have shown the streamlines in several conventional and non-conventional wing planforms, in an incompressible and stationary flow over the range of low Reynolds number. The authors will present the results obtained in several configurations (delta wings, winglets, box-wing). These experimental results have been used in the preliminary design of non-conventional wing planforms. This tool for aerodynamic design has been applied to the process of developing and building of an UAV which the authors have carried out.

This paper also describes in detail the main characteristics of the visualization technique, both in the water channel and in the model. The complete set of experimental visualization results carried out in the facility is presented and it is compared with the same configuration tested in a wind tunnel. This configuration will be a box-wing lay-out one. Finally, the conclusions the authors have reached, regarding stall conditions, are put forward.

1. Introduction

1.2 Review of the state of the art

It cannot be considered to be a novelty the use of smoke or ink to visualize the qualitative behavior of liquid or gas flows on different moving bodies. These techniques are relatively easy to carry out as well as economically affordable. The paradigmatic example of this was Reynold's experiment, which originated the characterization of laminar and turbulent flow in pipes.

Several types of measurements of drag on circular cylinders were carried out made by [2] in a stream with the Reynolds number range 0.5-100. Comparisons were made with other experimental values and theoretical calculations.

There are several outstanding papers and books which present a rigorous compendium of flow visualization techniques [1], [3], [4], [5], [7], [10], [11], [13], [12].

(Head) [6] developed flow visualization studies of the of the zero pressure gradient turbulent boundary layer over Reynolds number range $500 < Re < 17500$. These studies are focused on the nature of the hairpin vortex that appears in the different Re regime.

(Clayton & Massey) [3] reviewed all the principal techniques of flow visualization in water. They took into account the possibility of obtaining quantitative information from them.

(Werlé) [4] also published a paper summarizing the principal methods of flow visualization in liquids and gases.

It will be interesting to highlight the investigations about flow visualization techniques that are suited for studying unsteady flows [8, 9].

We can also find some interesting and rigorous works about flow visualization experiments on the flow on delta wing. Lowson's [17] works on a delta wing flow over the range $3000 < Re < 30000$ stand out.

It's really interesting to notice the large number of papers about investigations over visualization related to different wing planforms. The most outstanding ones are: [14], [15], [16], [17], [18], [19], [20], [21], [22], [23], [24], [25], [26], [27], [28].

This research is part of our design and build project of an UAS [29, 30]. The authors are testing several unconventional planform in order to improve aerodynamic design, basically based on box-wing configuration and winglet. The principles of winglets are explained in [31], [32], [33], [34], [35]. Many interesting investigations are focused on winglet and wingtips geometrical variations, such as [36], [37], [38], [39], [40].

However, there are not many directly applied to UAS, although we can highlight [41], [42], [43], and [44].

1.3 Flow visualization

Flow visualization allows, in some occasions, to discover phenomena that would not have been possible to know with point to point measurement techniques like hot wire anemometry or laser Doppler anemometry.

Dye visualization is one of the easiest to carry out, but it is not so easy to run it properly. The technique requires a correct selection of the dye class (properties, level of buoyancy, colour, etc.) and the proper position of the holes or needles over the surface model.

It is also important that the temperature difference between the dye or dye mixture and the working fluid (water, in this facility) is kept to a minimum; a large difference will lead to undesirable effects (buoyancy or convective ones).

Determining the amount of the dye solution level (usually with alcohol, or even water) became a very demanding task (a much time consuming job) and some degree of personal judgement by the authors. It is necessary to balance the concentration of dye; a thin dye will give a poor contrast, but a too much concentrated dye will obscure some details.

The selection of the dye fluid should have a specific gravity close to 1, and in most cases does not require adding another solvent. Another important characteristic will be that it shouldn't contaminate the water.

A traditional liquid selected for visualization in water was milk. It has high reflective properties which help to contrast the flow image quality. Its high fat content helps to retard the diffusion of the dye easily. Nevertheless, the milk could may curdle and block all the injection system.

The authors have also experienced with other visualization techniques such as hydrogen bubbles in water, and smoke tunnel and tufts over aerodynamic surfaces in air techniques.



Figure 1: Several examples of visualization techniques carried out by the authors. From left to right, tufts in a zero sweep wing with winglet at 20° alpha, slotted flap in a smoke tunnel, and velocity profile in a hydrogen bubbles apparatus.

2. Experimental apparatus

The hydrodynamic water channel is a parallelepiped formed by methacrylate panels joined together by special adhesive and fasteners. The dimensions are 3000x410x410 mm. The channel was reinforced by anodized aluminium profiles around the whole perimeter.



Figure 1: Water channel. General view.

An AC engine is used to move the belt of the driving system. The belt drags the model car transmitting the movement through a longitudinal arm.

The engine permits the model displacement in both directions, being adjustable in a wide range of velocities the forward movement; the velocity backwards is a fixed value.

The control system is placed in an electrical housing that isolates the complete electric systems from water influence. The speed regulation is done through a potentiometer that controls the engine frequency between 0 and 155Hz.



Figure 2: Electrical housing

The driving mechanism includes an end of stroke stop.

There are several controls for the following commands/buttons: switch ON/OFF, forward/backward movement, stop, emergency (shut off) and emergency stop light.



Figure 3: Electrical driving engine

The model support is a mobile structure formed by an inverted car, with four wheels that slide over the rails of the water channel's upper structure. Two horizontal plates (upper and lower ones), joined together by modular aluminium strut profiles, provide the adequate rigidity.

In order to improve the surrounding lighting, the apparatus included a set of halogen lights, due to their high brightness and low cost.



Figure 4: Model and camera support

The model holder arm and the camera holder arm are fixed to the upper structure. It allows taking high quality pictures in frontal/rear position, and an aerial one.

The ink tank, with a small peristaltic pump, is placed on the upper part of the car.

The model holder arm must turn around its position; with this turn, it's possible to take the model off the water to make modifications about test configurations. This one is a photographic ball-and-socket joint, to achieve the mentioned movements. We opted for a high performance (softness, strength) monopod photographic accessory, with a 3D ball-and-socket joint 391RC2 Manfrotto.

With the performance of the monopod element, we can lift up the model in a horizontal position out of the water. Thus, we can manipulate it out of the water. This one allows taking photos exactly from the same place, with the same perspective, so we could compare them. This arm has a fixed position, having only one joint like the model holder one to join it to the quick-release support. The quick-release support has a universal screw for any type of cameras.

The arm is formed by several aluminium strut profiles of different lengths, forming between them angles of nearly 90°. This is a solid union but we lose 2 degrees of freedom. By the way, the aluminium profiles are easily adjustable and quick mounting ability.

The channel has wheels that make it easier to move.

The channel filling is done through a flexible hose that communicates the intake with the intern circuit of the channel; it's in the lower part. 20 minutes are needed to fill it completely. Once the water level required to make the tests runs is reached, it's very important to close the stopcock in the bottom part of the channel, to avoid the water to going down due to its own pressure. For emptying it we use the same system, except for the fact that the flexible hose is now connected to the drainpipe. Besides, a water pump is used to speed up the process. The channel has a 1000 litter capacity; emptying it without the pump would take around 60 minutes f, and during that time the channel would be inoperative. The pump reduces the time of the process to 25 minutes.

The pump is situated on the lower part of the channel structure; it is basically a pump with a voltage regulator that permits to adjust the emptying speed.

2.1 Channel applications

The facility described above is appropriate for the study of rectilinear motion of the models with low velocities. The best choice is to use it to the investigation of stationary one-dimensional motion at low Reynolds number. Because of the incorporation of rotational motion equipment that provides rotating motion to the model it can be applied to 2D or 3D movements (propellers and rotors).

The channel has been used to the visualization of certain fluids and its quantitative analysis. Some of the tests made have been the following ones: Von Karman Vortex Street, flow around a propeller (2/3 bladed), vortex generation over wings with several geometries.

2.2 Types of tracer inks

It is interesting to bear in mind that no matter how different the models are, the method is always very similar. This consists of injecting the ink either through little tubes that located in the required position in the flow or intern injection through little holes on the surface of the model. In both cases, it is not possible to avoid completely the alterations that the mere presence of these injectors produces in the flow. This aspect is one of the main objectives to eliminate throughout every test runs; Trying to minimize the dimensions of the elements that are immerse in the flow has taken around 80% of the total number of hours dedicated to the experimental procedure.

An important point to be emphasized, as it has been enunciated before, is the fact that the ink tracer must become a constitutive part of the flow, it without discontinuity. The purpose of this is that the tracer liquid follows the flow. Because of that, the optimum tracer ink is the one that fulfils the following conditions:

- Low miscibility with the fluid: Implies a high value of surface tension, to avoid the possibility of being mixed completely with the fluid. With this feature, a major clarity in the patterns of flow will be achieved.
- Equal density between tracer and fluid: This characteristic avoids the tracer to move vertically by lack of hydrostatic balance.
- To have a high contrast with the channel's flow, it's essential to have a good visualization.
- Kinematic viscosity with a nearly value to water, to avoid forming velocity gradients, that create a velocity field that doesn't represent the desired flow pattern.
- It has to be neutral and easy to clean and to eliminate: This is a necessary feature in order to not to damage the channel (made of methacrylate) and to favour the channel cleaning after each test run.

In the following table, we resume the main performances of the tracers tested in our facility:

Table 1: Different types of tracer tested in the experiments

Tracer	Colour	% solution	Observations
Indian ink	Varied		It is not compatible with watery solutions
Watercolour	Varied		Too dense
Liquid colorant and colour concentrate	Varied	1-2 pills/liter	It is not compatible with watery solutions
Dental plaque detector	Red		It is necessary to grind it first. Very expensive.
Milk + alcohol + colouring	Varied	10% in water	It is complicated to obtain. No buoyancy.
Water based dye 1	Red	2-4% in water	It leaves oily trace
Water based dye 2	Black	10% in water	Foaming, it leaves trace
Blue food colouring	Blue	2-4% in water	Slightly thicker than water. No toxic.
Red food colouring	Red	2-4% in water	Slightly thicker than water. No toxic.
Yellow food colouring	Yellow	2-4% in water	Slightly thicker than water. No toxic.
Potassium permanganate	Purple	1% in water	It oxidizes shortly
Methylene blue	Blue	1% in water	Lack of opacity
Nigrosin	Black	1% in water	Very opaque. It has to rest before using
Rhodamine	Fluorescent violet	0,25-1% in water	Very luminous. High refraction index
Fluorescein	Fluorescent green	0,25-1% in water	Very luminous. High refraction index

With all these data gathered, we chose a tracer with an ink compound of a water solution of: potassium permanganate 1%, methanol for special application in ink mixtures, and adding 0,1g of sodium chloride, to reduce the ink dispersion.

It is remarkable to say that, if the ink injection is not done in the appropriate conditions, no tracer ink will follow the correct flow pattern. To avoid this inconvenience following aspects need to be kept in mind:

- The ink velocity must not have any perpendicular component to the model's surface. If this situation should occur, the ink should show a wrong surface visualization, since we would be adding additional velocity to the tracer liquid, in addition to energizing the boundary layer of the model.
- The injection has to be made in laminar regime through low turbulence injectors.

In the adjustment process of the model-camera system, it was necessary to correlate the car speed with the frequency regulator of the electric motor. We obtained this linear relationship:

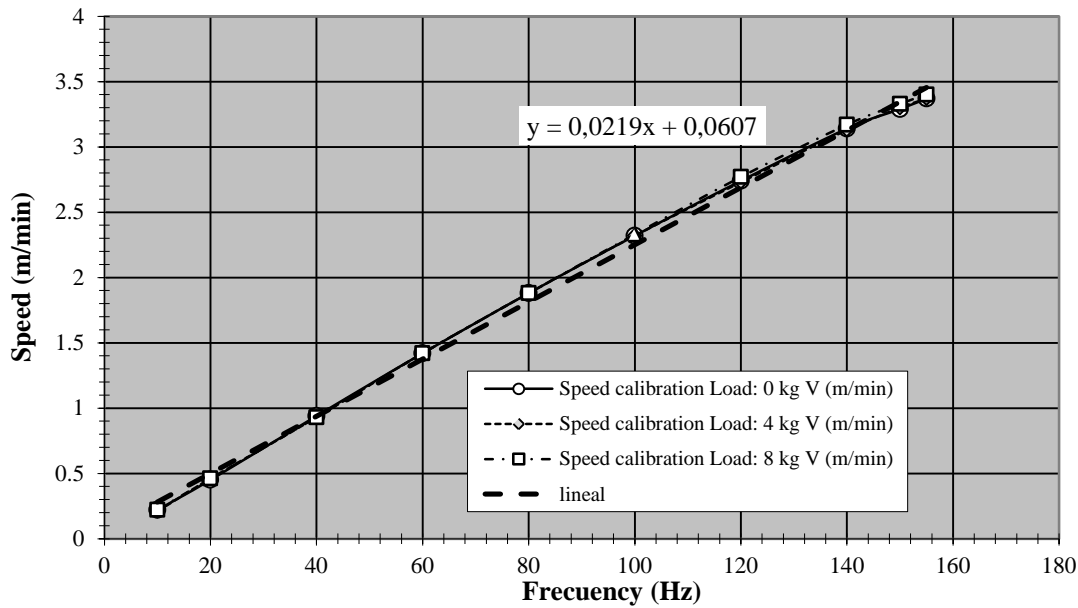


Figure 5: Model car speed versus electric DC converter.

3. Experimental procedure

To achieve correct flow visualization around different wing geometries studied along these tests a complete analysis of all the parameters that have influence on them was required. A thorough analysis of the design of the experimental conditions, the design of the building process of the model, with the position and amount of the injectors, among others, will lead to successful test results.

The main parameters to take into account in the flow visualization planning should be:

- Static pressure (point of injection): The static pressure is the result of the addition of the atmospheric pressure and the hydrostatic pressure caused by the height difference between the filling level of the ink deposit and the ink injection point. The value of the hydrostatic pressure can be modified raising the filling level of the tank, or raising the tank. It is important that the tubes that inject the ink to the tube sewer go decreasing in height because of this reason.
- Ink density: The ink tracer density should be closer to the water's density, as well as it should have an adequate contrast level with the channel wall colors.
- Vibrations' level: It's an essential parameter to take into account in order to obtain a clean visualization in a laminar regime. The whole set of the model/camera car must be correctly balanced, and its displacement must be as smooth as possible; all the rolling parts should be in an adequate greased state. After filling the channel, it will be necessary to wait for about 5 to 10 minutes, to assure the calm on the fluid.
- Ink volume of flow: The ink volume of flow is a basic parameter to achieve a proper visualization of flow, otherwise it's quite difficult to adjust. There are several ways to regulate the volume of flow: though a valve, modifying the head loss of the pipe (increasing the pipe length or decreasing the pipe diameter).
- Pumping dynamic pressure. Increasing pump voltage, we will increase the ink volume of flow in a quasi-linear way.
- Position of the needles. Once the aspects above have been improved, it is time to focus on the needles position as a main aspect to improve the flow visualization. It will require a theoretical analysis for taking decisions about best locations or zones to place the needles. In several occasions, it is not an easy task, because in certain tests the needles are installed inside the models. The geometry of the needles used in the experiments also will be considered; features like the edge, length and diameter should modify the speed flow and the quality of the ink jet.
- Others parameters must be taken into account such as: speed model car (frequency DC converter), spatial orientation (angles) of the model, Reynolds number (proportional to model characteristic length), and its weight.

4. Tests results

In this section a set of experimental results with several wing models will be shown.

1. We begin with a low aspect ratio wing research. The experimental data were: $\alpha=30^\circ$, $Re=1000$ (based on mean chord of the wing). The last one was developed with a yaw angle $\beta=10^\circ$ and roll angle $\phi=30^\circ$. Low wing aspect ratio wing with LEX (leading-edge extensions) tests were also carried out.

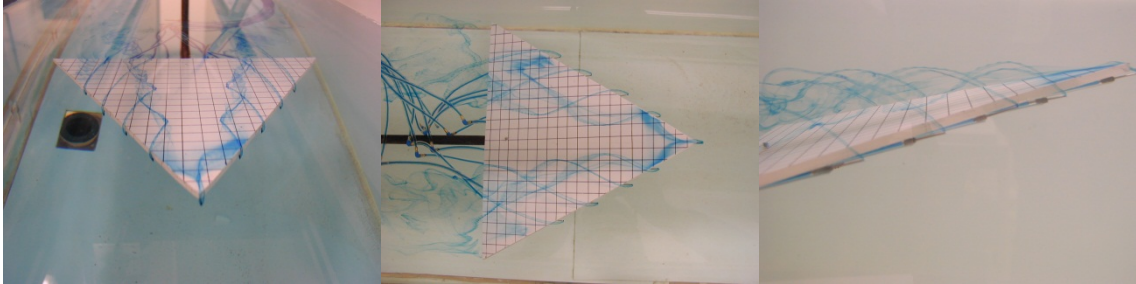


Figure 6: Low aspect ratio delta wing experimental results. $Re=1000$, $\alpha=30^\circ$, $\beta=0^\circ$, $\phi=0^\circ$.

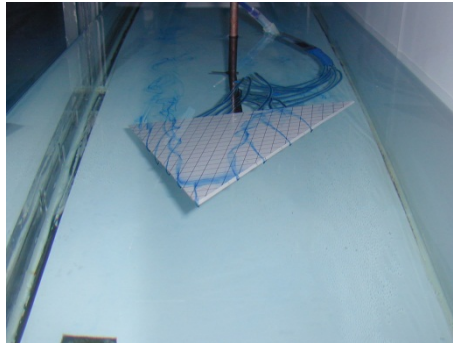


Figure 6: Low aspect ratio delta wing experimental results. $Re=1000$, $\alpha=30^\circ$, $\beta=10^\circ$, $\phi=30^\circ$.

2. Low wing aspect ratio wing with LEX (leading-edge extensions) tests were also carried out.

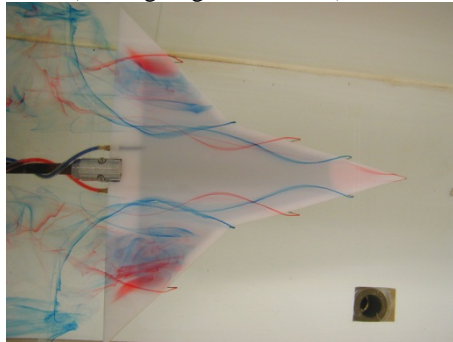


Figure 7: Low aspect ratio delta wing with LEX experimental results. $Re=1300$, $\alpha=30^\circ$, $\beta=0^\circ$, $\phi=0^\circ$.

3. Winglets visualization. A set of 30 different configuration tests were carried out. Several needle positions, with three speeds of the model car, and three angles of attack were studied. The needle position related to the wing surface was tested: completely out of the leading edge of the model, with the bezel of the needles flushing of the leading edge, and finally with the needles completely hiding in the model.



Figure 8: Winglet visualization. $Re=1300$, $\alpha=0^\circ$, $\beta=5^\circ$, $\phi=0^\circ$.

5. Conclusions

This paper presents the main results obtained in a water channel flow visualization facility. It allows having a conceptual idea about flow over wing configurations, or a wide variety of flow geometries.

This technique is an appropriate one to show the nonlinear behavior of LAR wings (low aspect ratio) with flat-plate wing. It should be a field of application for UAS. Polhamus [49] leading-edge-suction analogy suggested the following equation for lift coefficient:

$$C_L = K_p \sin \alpha \cos^2 \alpha + K_v \cos \alpha \sin^2 \alpha \quad (1)$$

He concluded that the total force (before stall) is given by an addition of potential lift (linear with α) and a vortex lift associated with the separated vortex cores; the flow visualization shows the vortex over sharp leading edges. K_p depends on the aspect ratio, sweep angle and leading shape [50].

Lamar [51] proposed a nonlinear equation for the drag coefficient and for the pitching moment with a similar structure with (1).

Many of recent concepts of wing planform optimization may lead to reduce induced-drag coefficient (drag due to lift) [31]. Drag due to lift has basically a highly tridimensional origin. It has a dominant effect in low speed drag. There are several ways to improve induced drag. One of the most cited approaches to induced drag reduction is the application on nonplanar lifting surfaces, such as winglets. In this sense, flow visualization over winglet was carried out in this research.

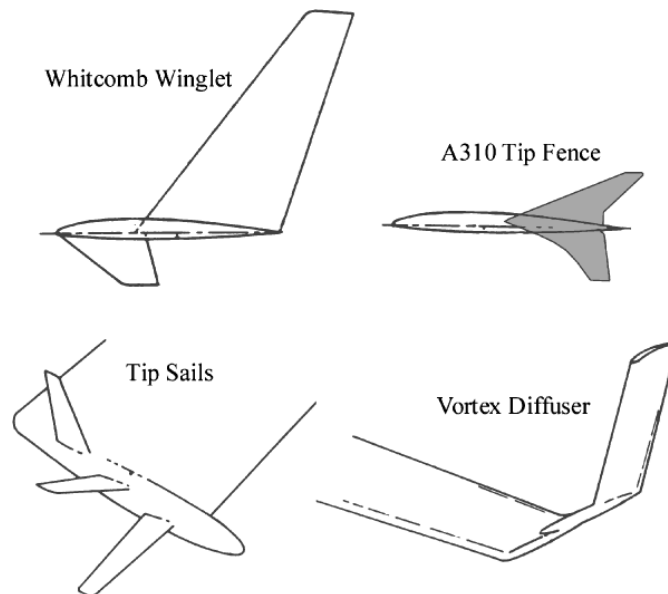


Figure 9: Winglet and wing tip device geometries. From [32]

References

- [1] Tietjens, O. K. G., & Prandtl, L. (1957). *Applied hydro-and aeromechanics: based on lectures of L. Prandtl* (Vol. 2). Courier Dover Publications.
- [2] Tritton, D. J. (1959). Experiments on the flow past a circular cylinder at low Reynolds numbers. *J. Fluid Mech*, 6(4), 547-567.
- [3] Clayton, B. R., & Massey, B. S. (1967). Flow visualization in water: a review of techniques. *Journal of Scientific Instruments*, 44(1), 2.
- [4] Werle, H. (1973). Hydrodynamic flow visualization. *Annual Review of Fluid Mechanics*, 5(1), 361-386.
- [5] Van Dyke, M., & Van Dyke, M. (1982). *An album of fluid motion*.
- [6] Head, M. R., & Bandyopadhyay, P. (1981). New aspects of turbulent boundary-layer structure. *J. Fluid Mech*, 107, 297-338.
- [7] Merzkirch, W. (1987). *Flow visualization*. Academic Press.
- [8] Gad-el-Hak, M. (1987). The water towing tank as an experimental facility. *Experiments in fluids*, 5(5), 289-297.
- [9] Gad-El-Hak, M. (1988). Visualisation techniques for unsteady flows: an overview. *J. Fluids Engng.*, 110 (1988), p. 231 (Sept.) [13 pp., 103 ref., 16 fig.]
- [10] Yang, W. J. (1989). *Handbook of flow visualization*. New York, Hemisphere Publishing Corp., 1989, 687 p. Volume 1.
- [11] Freymuth, P. (1993). Flow visualization in fluid mechanics. *Review of scientific instruments*, 64(1), 1-18.
- [12] Perry, A. E., Chong, M. S. (2000). Interpretation of flow visualization. *Flow Visualization: Techniques and Examples*, 1-26.
- [13] Smits, A. J., & Lim, T. T. (2000). *Flow visualization: techniques and examples* (Vol. 1). London, UK: Imperial College Press.
- [14] Niedenfuhr, F. W., Leissa, A. W., Gad-El-Hak, M., & Blackwelder, R. (1985). The discrete vortices from a delta wing. *AIAA journal*, 23(6), 961-962.
- [15] Freymuth, P., Bank, W., & Finaish, F. (1987). Further visualization of combined wing tip and starting vortex systems. *AIAA journal*, 25(9), 1153-1159.
- [16] Payne, F. M., Ng, T., Nelson, R. C., & Schiff, L. B. (1988). Visualization and wake surveys of vortical flow over a delta wing. *AIAA journal*, 26(2), 137-143.
- [17] Lawson, M. V. "Visualization measurements of vortex flows", *Journal of Aircraft*, Vol. 28, No. 5 (1991), pp. 320-327. doi: 10.2514/3.46030.
- [18] Freymuth, P. (1993). Vortex topology of rectangular wings in pictures, sketches, and conjectures. *Journal of Flow Visualization and Image Processing*, 1(1).
- [19] Cotton, Stacey J., Bjarke, Lisa J. (1994). Flow-Visualization Study of the X-29A Aircraft at High Angles of Attack Using a 1/48-Scale Model. NASA Technical Memorandum 104268.
- [20] Lawson, M.V., Riley, A. J. (1995) Vortex breakdown control by delta wing geometry. *Journal of Aircraft* 32:4, 832-838.
- [21] Ol, M., Gharib, M. "Leading-Edge Vortex Structure of Nonslender Delta Wings at Low Reynolds Number," *AIAA Journal*, Vol. 41, 2003, pp. 16–26.
- [22] Yaniktepe, B., and Rockwell, D., "Flow Structure on a Delta Wing of Low Sweep Angle," *AIAA Journal*, Vol. 42, 2004, pp. 513–523. doi:10.2514/1.1207
- [23] Yaniktepe, B., and Rockwell, D., "Flow Structure on Diamond and Lambda Planforms: Trailing-Edge Region," *AIAA Journal*, Vol. 43, 2005, pp. 1490–1512.
- [24] Gursul, I. "Review of Unsteady Vortex Flows over Slender Delta Wings", *Journal of Aircraft*, Vol. 42, No. 2 (2005), pp. 299-319.
- [25] Gursul, I., Gordnier, R., Visbal, M. Unsteady aerodynamics of nonslender delta wings, *Progress in Aerospace Sciences*, Volume 41, Issue 7, October 2005, Pages 515-557, ISSN 0376-0421, 10.1016/j.paerosci.2005.09.002.
- [26] Gordnier, R. E., Visbal, M. R., Gursul, I., and Wang, Z., "Computational and Experimental Investigation of a Nonslender Delta Wing," *AIAA Journal*, Vol. 47, No. 8, Aug. 2009, pp. 1811–1825.
- [27] Sahin, B., Yayla, S., Canpolat, C., Akilli, H. (2012). Flow structure over the yawed nonslender diamond wing. *Aerospace Science and Technology* 23:1, 108-119.
- [28] Canpolat, C., Yayla, S., Sahin, B., Akilli, H. (2012). Observation of the Vortical Flow over a Yawed Delta Wing. *Journal of Aerospace Engineering* 25:4, 613-626.
- [29] Barcala Montejano, M. A., Gandia Agüera, F., Rodríguez Sevillano, A., Crespo Moreno, J., Pérez Álvarez, J., Gómez Pérez, J. P., & Gómez Pérez, I. (2010). The Application of Rapid Prototyping in the Design of an UAV. *ICAS 2010. 27th International Congress of the Aeronautical Sciences*.
- [30] Barcala M, Cuerno-Rejado C, del Giudice S, Gandía-Agüera F, Rodríguez-Sevillano, AA. Experimental investigation on box-wing configuration for UAS. *26th Bristol International Unmanned Air Vehicle Systems Conference*, University of Bristol, 11-13 April 2011.

- [31] Gall, P.D. An experimental and theoretical analysis of the aerodynamic characteristics of a biplane-winglet configuration. NASA TM 85815, 1984.
- [32] Kroo, I. (2001). Drag due to lift: concepts for prediction and reduction. *Annual Review of Fluid Mechanics*, 33(1), 587-617.
- [33] Ning, S. A., Kroo, I. (2008). Tip extensions, winglets, and c-wings: conceptual design and optimization. *AIAA Paper*, 7052.
- [34] Ning, A., Kroo, I. (2010). Multidisciplinary considerations in the design of wings and wing tip devices. *Journal of Aircraft*, 47(2), 534-543.
- [35] Hicken, J. E., Zingg, D. W. (2010). Induced-Drag Minimization of Nonplanar Geometries Based on the Euler Equations. *AIAA journal*, 48(11), 2564-2575.
- [36] Smith, M. J., Komerath, N., Ames, R., Wong, O., Pearson, J. (2001). Performance analysis of a wing with multiple winglets *AIAA-2001-2407*.
- [37] Prithvi, R. A., Hossain, A., Jaafar, A. A., Edi, P., Younis, T. S., Saleem, M. (2005). Drag reduction in aircraft model using elliptical winglet. *Journal of IEM, Malaysia*, 66(4), 1-8.
- [38] Nazarinia, M., Soltani, M. R., & Ghorbanian, K. (2006). Experimental study of vortex shapes behind a wing equipped with different winglets. *Journal of Aerospace Science and Technology*, 3(1), 1-15.
- [39] Coiro, D., Nicolosi, F., Scherillo, F., & Maisto, U. (2008). Single Versus Multiple Winglets: Numerical and Experimental Investigation. In *Proceedings of XXVI ICAS Congress* (pp. 2008-2).
- [40] Miklosovic, D. S. (2008). Analytic and experimental investigation of dihedral configurations of three-winglet planforms. *Journal of fluids engineering*, 130(7).
- [41] Elkhoury, M., Rockwell, D. "Visualized Vortices on Unmanned Combat Air Vehicle Planform: Effect of Reynolds Number", *Journal of Aircraft*, Vol. 41, No. 5 (2004), pp. 1244-1247.
- [42] Ol, M. V., "Water Tunnel Velocimetry Results for the 1303 UCAV Configuration," *AIAA Paper 2006-2990*, 2006.
- [43] Coiro, D. P., Nicolosi, F., Scherillo, F., Maisto, U. (2008). Improving Hang-Glider Maneuverability Using Multiple Winglets: A Numerical and Experimental Investigation. *Journal of Aircraft*, 45(3), 981-989.
- [44] Sherer, S. E., Visbal, M. R., Gordnier, R. E., Yilmaz, T. O., Rockwell, D. O. "1303 Unmanned Combat Air Vehicle Flowfield Simulations and Comparison with Experimental Data", *Journal of Aircraft*, Vol. 48, No. 3 (2011), pp. 1005-1019.
- [45] Lim, T. T., & Nickels, T. B. (1995). Vortex rings. In *Fluid vortices* (pp. 95-153). Springer Netherlands.
- [46] Gad-El-Hak, M., Ho, C. M. Unsteady flow around an ogive cylinder. *Journal of Aircraft*, June 1986, Vol. 23, No. 6 : pp. 520-528. (doi: 10.2514/3.45338).
- [47] Potts, J. R., Crowter, W. J. Visualisation of the Flow over a Disc-Wing. 9th. International Symposium on Flow Visualization, 2000. Edinburgh, Scotland, UK. August 22-25, 2000. Paper number 247 247-1.
- [48] Bakić, V. and Perić, M. Visualization of Flow Around Sphere for Reynolds Numbers between 22000 and 400000. *Thermophysics and Aeromechanics*, 2005, Vol. 12, No. 3.
- [49] Polhamus, E. C. (1971). Predictions of vortex-lift characteristics by a leading-edge suction analogy. *Journal of Aircraft*, 8(4), 193-199.
- [50] Mueller, T. J., Kellogg, J. C., Ifju, P. G., & Shkarayev, S. V. (2007). Introduction to the design of fixed-wing micro air vehicles: including three case studies. *American Institute of Aeronautics and Astronautics*.
- [51] Lamar, J. E. (1976). Prediction of vortex flow characteristics of wings at subsonic and supersonic speeds. *Journal of Aircraft*, 13(7), 490-494.